

## Thermal Conductivity and Viscosity Measurements of Water-Based TiO<sub>2</sub> Nanofluids

A. Turgut · I. Tavman · M. Chirtoc ·  
H. P. Schuchmann · C. Sauter · S. Tavman

Received: 9 October 2008 / Accepted: 12 May 2009 / Published online: 10 June 2009  
© Springer Science+Business Media, LLC 2009

**Abstract** In this study, the thermal conductivity and viscosity of TiO<sub>2</sub> nanoparticles in deionized water were investigated up to a volume fraction of 3 % of particles. The nanofluid was prepared by dispersing TiO<sub>2</sub> nanoparticles in deionized water by using ultrasonic equipment. The mean diameter of TiO<sub>2</sub> nanoparticles was 21 nm. While the thermal conductivity of nanofluids has been measured in general using conventional techniques such as the transient hot-wire method, this work presents the application of the  $3\omega$  method for measuring the thermal conductivity. The  $3\omega$  method was validated by measuring the thermal conductivity of pure fluids (water, methanol, ethanol, and ethylene glycol), yielding accurate values within 2 %. Following this validation, the effective thermal conductivity of TiO<sub>2</sub> nanoparticles in deionized water was measured at temperatures of 13 °C, 23 °C, 40 °C, and 55 °C. The experimental results showed that the thermal conductivity increases with an increase of particle volume fraction, and the enhancement was observed to be 7.4 % over the base fluid for a nanofluid with 3 % volume fraction of TiO<sub>2</sub> nanoparticles at 13 °C. The increase in viscosity with the increase of particle volume fraction was much more than predicted by the Einstein model. From this research, it seems that the increase in the nanofluid viscosity is larger than the enhancement in the thermal conductivity.

---

A. Turgut · I. Tavman (✉)  
Mechanical Engineering Department, Dokuz Eylul University, 35100 Bornova Izmir, Turkey  
e-mail: ismail.tavman@deu.edu.tr

M. Chirtoc  
Thermophysics Laboratory, GRESPI, University of Reims, BP 1039, 51687 Reims Cedex 2, France

H. P. Schuchmann · C. Sauter  
University Institute of Food Process Engineering, University of Karlsruhe, Karlsruhe 76131, Germany

S. Tavman  
Food Engineering Department, Ege University, 35100 Bornova Izmir, Turkey

**Keywords**  $3\omega$  method · Nanofluid · Nanoparticle · Thermal conductivity · Titanium dioxide · Viscosity

## 1 Introduction

Nanofluids are liquid suspensions of particles with at least one of their dimensions smaller than 100 nm. After the pioneering work of Choi [1], nanofluids become a new class of heat transfer fluids. Their potential benefits and applications in many industries from electronics to transportation have attracted great interest from many researchers both experimentally and theoretically. Efforts in research in the nanofluids area has increased annually since 1995; more than 450 nanofluid-related research papers were published in *Science Citation Index* journals. Very recent papers [2,3] provide a detailed literature review of nanofluids including synthesis, potential applications, and experimental and analytical analysis of effective thermal conductivity, effective thermal diffusivity, and convective heat transfer.

Published results show an enhancement in the thermal conductivity of nanofluids, in a wide range even for the same host fluid and same nominal size or composition of the additives. Since this enhancement can not be explained with the existing classical effective thermal-conductivity models, such as the Maxwell [4] or Hamilton–Crosser [5] models, this also motivates a wide range of theoretical approaches for modeling these thermal phenomena. Reported results show that the particle volume concentration, particle material, particle size, particle shape, base fluid material, temperature, additive, and acidity play an important role in enhancement of the thermal conductivity of nanofluids.

The effect of the fluid temperature on the effective thermal conductivity of nanoparticle suspensions was first presented by Masuda et al. [6]. They reported that for water-based nanofluids, consisting of  $\text{SiO}_2$  and  $\text{TiO}_2$  nanoparticles, the thermal conductivity was not much more temperature dependent than that of the base fluid. Contrary to this result, Das et al. [7] observed a two-to-four fold increase in the thermal conductivity of nanofluids, containing  $\text{Al}_2\text{O}_3$  and  $\text{CuO}$  nanoparticles in water, over a temperature range of 21 °C to 51 °C. Several groups [8–14] reported studies with different nanofluids, which support the result of Das et al. [7]. For the temperature dependence of the relative thermal conductivity (ratio of effective thermal conductivity of nanofluids to thermal conductivity of base fluid), although a major group of publications showed an increase with respect to temperature, some of the other groups observed a moderate enhancement or temperature independence [6,15–18].

Since viscosity is a fundamental characteristic property of a fluid that influences flow and heat transfer phenomena, determining the viscosity of nanofluids is necessary for optimizing pumping costs of heat transfer applications. There are some studies on the viscosity of nanofluids [6,19–22], but compared with the experimental studies on thermal conductivity, they are limited. These reports show that the viscosity of nanofluids increased anomalously with increasing particle concentration, and it is not possible to predict this by classical models such as those of Einstein [23] or Nielsen [24]. To draw a clear conclusion, more experimental research is needed for both the thermal conductivity and viscosity of nanofluids.

In this article we report experimental measurements of the effective thermal conductivity using the  $3\omega$  method and the effective viscosity using the vibro-viscometer for TiO<sub>2</sub>-water nanofluids, at temperatures from 13 °C to 55 °C. We compare our results with those in the literature. The results show that the effective thermal conductivity of nanofluids increases as the volume fraction of the particles increases but not anomalously as indicated in the majority of the literature, and this enhancement is very close to that predicted by the Hamilton–Crosser model [5]. We also concluded that the relative thermal conductivity is not temperature dependent for TiO<sub>2</sub>-water nanofluids. The viscosity measurements show that, as the temperature increases, the viscosity of the nanofluids investigated here decreases exponentially the same as the base fluid, and the relative viscosity is dependent on the volume fraction of the nanoparticles.

## 2 Experimental

### 2.1 Production and Dispersion Characteristics of TiO<sub>2</sub>-Water Nanofluids

A two-step method was used to produce TiO<sub>2</sub> water-based nanofluids with concentrations of TiO<sub>2</sub> nanoparticles from 0.2 vol% to 3 vol%, without any surfactant. In the first stage, dry TiO<sub>2</sub> (Aeroxide<sup>®</sup> (P25)) nanoparticles, with an average primary particle size of 21 nm in diameter and specific surface area (BET) of  $(50 \pm 15) \text{ m}^2 \cdot \text{g}^{-1}$ , manufactured by Degussa Co. were mixed in de-ionized water. The next step was to homogenize the mixture using ultrasonic vibration (UIP 1000S, Dr. Hielscher GmbH) to break down the agglomerations.

### 2.2 Measurements of the Effective Thermal Conductivity

The effective thermal conductivity of nanofluids was measured by a technique based on a hot-wire thermal probe with ac excitation and  $3\omega$  lock-in detection. Since the principle and procedures of the technique have been described in detail previously [25, 26], only a brief description is given here. We consider a thermal probe (ThP) consisting of a metallic wire of length  $2l$  and radius  $r$  immersed in a liquid sample, acting simultaneously as a heater and as a thermometer. The sample and probe thermophysical properties are the volumetric specific heat  $\rho c$  and thermal conductivity  $k$ , with the respective subscripts (s) and (p). The wire is excited by an ac current at a frequency  $f/2$ , and we assume that it is thermally thin in the radial direction so that the temperature  $\theta(f)$  is uniform over its cross section. Since the electrical resistance of the wire is modulated by the temperature increase, the voltage across the wire contains a third harmonic  $V_{3\omega}$  proportional to  $\theta(f)$ . It is convenient to use a normalized (reduced)  $3\omega$  signal,  $F(f)$  [27]. For  $r/\mu_s \ll 1$ , the temperature increase  $\theta(f)$  generated by a modulated line heat source  $P$  in an infinite and homogeneous medium can be approximated from Carslaw and Jaeger [28] and Cahill [29] by

$$F(f) \propto \theta(f) = -\frac{P/l}{2\pi k_s} \left( \gamma + \ln \frac{\sigma_s r}{2} \right) = -\frac{P/l}{2\pi k_s} \left( \ln \frac{1.26r}{\mu_s} + i \frac{\pi}{4} \right) \quad (1)$$

where  $\gamma = 0.5772$  is the Euler constant. The complex quantity  $\sigma_s$  is given by  $\sigma_s = (1 + i)/\mu_s = (i2\pi f/\alpha_s)^{1/2}$  where  $\mu_s$  is the thermal diffusion length at frequency  $f$  and  $\alpha_s = k_s/\rho_s c_s$  is the thermal diffusivity.

In this work we are concerned with the measurement of thermal properties of water-based nanofluids, relative to pure water (subscript w). From Eq. 1 one has

$$\frac{k_s}{k_w} = \frac{\text{Im}(F_w)}{\text{Im}(F_s)} \quad \text{and} \quad \cot \phi_s - \cot \phi_w = \frac{\sin(\phi_w - \phi_s)}{\sin \phi_s \sin \phi_w} = -\frac{2}{\pi} \ln \frac{\alpha_s}{\alpha_w} \quad (2)$$

For a small diffusivity difference, the phase yields

$$\frac{\alpha_s}{\alpha_w} = 1 + \frac{\pi(\phi_s - \phi_w)}{2 \sin^2 \phi_w} \quad (3)$$

In principle, Eq. 2 give frequency-independent results, but in practice there is an optimum frequency range such that  $r/\mu_s < 1$  in which  $k_s$  and  $\alpha_s$  have stable and low noise values as a function of frequency.

The first harmonic in the voltage signal is dominant and must be canceled by a Wheatstone bridge arrangement. The selection of the third harmonic from the differential signal across the bridge is performed by a Stanford SR850 lock-in amplifier tuned to this frequency, Fig. 1 [30]. The thermal probe (ThP) is made of Ni wire, 40  $\mu\text{m}$  in diameter and  $2l = 19.0$  mm long. The temperature amplitude  $\theta$  in water was 1.25 K. The minimum sample volume for Eq. 1 to apply is that of a liquid cylinder centered on the wire and having a radius equal to about  $3\mu_s$ . At  $2f = 1$  Hz, this amounts to 25  $\mu\text{L}$ . The method was validated with measurements on pure fluids (water, methanol, ethanol, and ethylene glycol), yielding accurate  $k$ -ratios within 2% (Eq. 2) and an absolute  $\alpha$  value for water within 1.5% (Eq. 3). Each thermal conductivity measurement was repeated five times and due to ac modulation

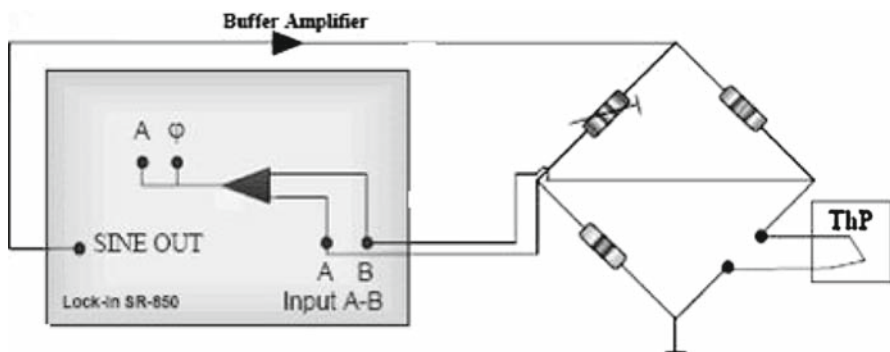
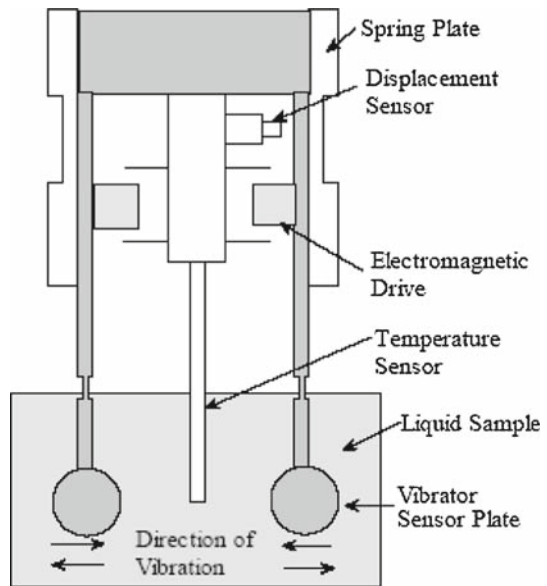


**Fig. 1** Experimental setup for  $3\omega$  hot-wire measurements consisting of thermal probe (ThP), Wheatstone bridge, lock-in amplifier, and buffer amplifier

**Fig. 2** Schematic diagram of the vibro-viscometer [31]



and lock-in signal processing, the reproducibility of absolute values is 0.3% in  $k$  [25,26].

### 2.3 Measurement of the Effective Viscosity

The experimental setup for measuring the effective viscosity of nanofluids, consists of a sine-wave Vibro Viscometer SV-10 and Haake temperature-controlled bath with a stability of 0.1 °C. The SV-10 viscometer (A&D, Japan), has two thin sensor plates that are driven with electromagnetic force at the same frequency by a sine-wave vibration in reverse phase like a tuning fork. The electromagnetic drive controls the vibration of the sensor plates to maintain a constant amplitude. The drive electric current, which is an exciting force, will be detected as the magnitude of the viscosity produced between the sensor plates and the sample fluid (Fig. 2 [31]). The coefficient of viscosity is obtained by the correlation between the drive electric current and the magnitude of the viscosity. Since the viscosity is dependent upon the temperature of the fluid, it is very important to measure the temperature of the fluid accurately. Using this viscometer we can determine an accurate temperature in a short period of time since the fluid and the detection unit (sensor plates) with small surface area/thermal capacity reaches thermal equilibrium in only a few seconds. The measurement range of viscosity is 0.3 mPa·s to 10,000 mPa·s.

The effective viscosities of TiO<sub>2</sub>–water nanofluids with concentrations from 0.2 vol% to 3 vol% were measured at temperatures from 13 °C to 55 °C.

### 3 Results and Discussion

#### 3.1 Effective Thermal Conductivity of TiO<sub>2</sub> Nanofluids

The effective thermal conductivity of TiO<sub>2</sub>–water nanofluids with concentrations of (0.2, 1.0, 2.0 and 3.0) vol% were measured at temperatures of 13 °C, 23 °C, 40 °C, and 55 °C. The comparison of our present results for the thermal-conductivity enhancement of TiO<sub>2</sub>–water nanofluids with the data of several groups from the literature is given in Table 1. From this comparison one can see that our results are at the lower end of the published data, both for volume fraction and temperature dependence.

Recently, we have reported experimental data for the relative thermal conductivity at room temperature (23 °C for our data), which shows good agreement with selected literature data (Fig. 3 [26]). Whereas other data show anomalous enhancement for the effective thermal conductivity of TiO<sub>2</sub>–water nanofluids, which can not be explained with classical models such as Maxwell [4], Hamilton–Crosser [5], or Bruggeman [37], from Fig. 4 it can be seen that our data show reasonably good agreement.

Bruggeman [37] proposed a model to analyze the interactions among randomly distributed particles by using the mean field approach

$$k_{\text{eff}} = \frac{1}{4} [(3\phi - 1)k_p + (2 - 3\phi)k_f] + \frac{k_f}{4}\sqrt{\Delta} \quad (4)$$

$$\Delta = [(3\phi - 1)^2 (k_p/k_f)^2 + (2 - 3\phi)^2 + 2(2 + 9\phi - 9\phi^2)(k_p/k_f)] \quad (5)$$

where  $\phi$  is the particle volume fraction of the suspension and  $k_f$  and  $k_p$  are the thermal conductivities of the base fluid and particles, respectively.

On the basis of the Maxwell model, Hamilton and Crosser presented a shape factor  $n$ , given by  $n = 3/\Psi$  with  $\Psi$  the sphericity;  $\Psi = 1$  for spherical particles:

$$\frac{k_{\text{eff}}}{k_f} = \frac{k_p + (n - 1)k_f - (n - 1)(k_f - k_p)\phi}{k_p + (n - 1)k_f + (k_f - k_p)\phi} \quad (6)$$

Xie et al. [38] derived an expression for calculating the enhanced thermal conductivity of nanofluid by considering the effects of the nanolayer thickness, nanoparticle size, volume fraction, and thermal conductivity ratio of particle to fluid. The expression is

$$k_{\text{eff}}/k_f = \left( 1 + 3\Theta\phi_T + \frac{3\Theta^2\phi_T^2}{1 - \Theta\phi_T} \right) \quad (7)$$

with

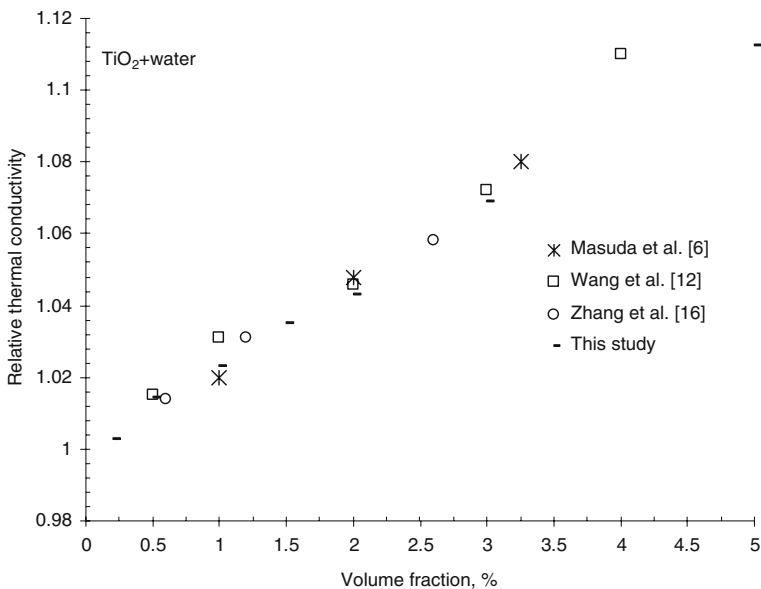
$$\Theta = \frac{\beta_{\text{lf}} [(1 + \gamma)^3 - \beta_{\text{pl}}/\beta_{\text{fl}}]}{(1 + \gamma)^3 + 2\beta_{\text{lf}}\beta_{\text{pl}}} \quad (8)$$

**Table 1** Comparison of thermal conductivity enhancement in TiO<sub>2</sub>–water nanofluids

Author	Nominal TiO <sub>2</sub> particle size (nm)	Volume fraction (%)	Thermal conductivity enhancement (%)	Reduced thermal conductivity enhancement and temperature	Measurement method
<i>(a) In the literature</i>					
Masuda et al. [6]	27	1.00	2.0	2.0 at 32 °C	Transient hot wire
		2.00	4.8	2.4 at 32 °C	
		3.25	8.0	2.5 at 32 °C	
		3.25	8.4	2.6 at 47 °C	
		3.10	7.5	2.4 at 87 °C	
		4.30	10.5	2.4 at 32 °C	
		4.30	10.8	2.5 at 47 °C	
		4.30	9.9	2.3 at 87 °C	
Wang et al. [12]	26	0.5	1.5	3.0 at 18 °C	3 $\omega$ method
		0.5	5.0	10.0 at 65 °C	
		1.0	3.1	3.1 at 18 °C	
		1.0	6.0	6.0 at 43 °C	
		1.0	10.0	10.0 at 65 °C	
		2.0	4.6	2.3 at 18 °C	
		2.0	8.4	4.2 at 43 °C	
		2.0	13.3	6.7 at 65 °C	
		4.0	11.0	2.8 at 18 °C	
		4.0	15.0	3.8 at 43 °C	
Zhang et al. [16]	40	0.6	1.4	2.3 at 10 °C	Transient short hot wire
		1.2	3.1	2.6 at 10 °C	
		2.6	5.8	2.2 at 10 °C	
		1.2	3.6	3.0 at 30 °C	
		2.6	5.4	3.0 at 30 °C	
		0.6	1.1	2.1 at 40 °C	
		1.2	3.7	3.1 at 40 °C	
		2.6	6.5	2.5 at 40 °C	
Yoo et al. [32]	25	0.1	10.0	100	Transient hot wire
		0.5	11.8	23.6	
		1.0	14.5	14.5	
He et al. [33]	21	0.24	1.9	7.9 at 22 °C	Transient hot wire
		0.6	3.6	6.0 at 22 °C	
		1.18	7.5	6.4 at 22 °C	
		1.92	8.6	4.5 at 22 °C	
Pak and Cho [34]	27	1.0	3.5	3.5	Transient hot wire
		2.0	5.0	2.5	
		3.0	7.7	2.6	
		4.0	12.0	3.0	
Murshed et al. [35]	15	0.5	4.5	9.0	Transient hot wire
		0.8	9.5	11.9	
		1.0	18.5	18.5	
		2.0	23.5	11.8	
		3.0	25.5	8.5	
		4.0	27.5	6.9	
	5.0	30.0	5.9		

**Table 1** continued

Author	Nominal TiO <sub>2</sub> particle size (nm)	Volume fraction (%)	Thermal conductivity enhancement (%)	Reduced thermal conductivity enhancement and temperature	Measurement method
Wen and Ding [36]	34	0.29	1.8	6.2	Transient hot wire
		0.41	3.1	7.6	
		0.53	5.1	9.6	
		0.68	6.3	9.3	
(b) From this study		0.2	0.4	2.0 at 13 °C	3 $\omega$ method
		1.0	2.5	2.5 at 13 °C	
		2.0	4.2	2.1 at 13 °C	
		3.0	7.4	2.5 at 13 °C	
		0.2	0.3	1.5 at 23 °C	
Present results	21	1.0	2.3	2.3 at 23 °C	3 $\omega$ method
		2.0	4.3	2.2 at 23 °C	
		3.0	6.9	2.3 at 23 °C	
		0.2	0.5	2.5 at 40 °C	
		1.0	2.7	2.7 at 40 °C	
		2.0	4.8	2.4 at 40 °C	
		3.0	7.1	2.4 at 40 °C	
		0.2	0.3	1.5 at 55 °C	
		1.0	2.2	2.2 at 55 °C	
		2.0	4.5	2.3 at 55 °C	
3.0	7.2	2.4 at 55 °C			

**Fig. 3** Experimental results of relative thermal conductivity of TiO<sub>2</sub> nanofluids, for room temperature (23 °C for our data), compared to selected literature data [26]



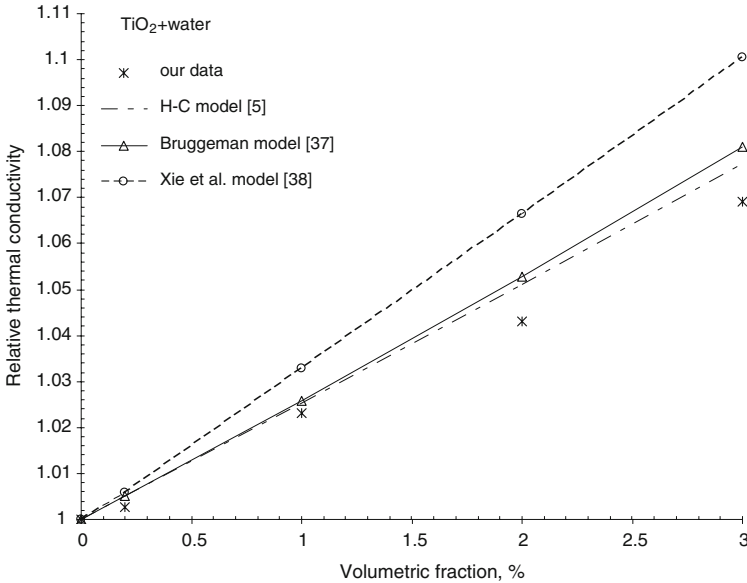


**Fig. 4** Experimental data for the relative thermal conductivity of TiO<sub>2</sub> nanofluids from this study, compared to models

where

$$\beta_{lf} = \frac{k_l - k_f}{k_l + 2k_f}, \quad \beta_{pl} = \frac{k_p - k_l}{k_p + 2k_l}, \quad \beta_{fl} = \frac{k_f - k_l}{k_f + 2k_l}$$

and  $\gamma = \delta/r_p$  is the ratio of the nanolayer thickness to nanoparticle radius.  $\phi_T$  is the modified total volume fraction of the original nanoparticle and nanolayer,  $\phi_T = \phi(1 + \gamma)^3$ . By choosing  $r_p = 10.5$  nm,  $\delta = 2$  nm, and the thermal conductivity of the nanolayer  $k_l = 2k_f$ , the Xie et al. [38] model gives a larger prediction than the H-C model and Bruggeman model (Fig. 4).

In the literature there are several papers [7–14] indicating that the thermal conductivity ratio of nanofluid to base fluid (relative thermal conductivity) increases with increasing temperature. For the case of water-based nanofluids containing TiO<sub>2</sub> spherical nanoparticles, there are few reports on the temperature dependence [6, 12, 16]. We compare our results with these data, for selected nanoparticle volumetric fractions between 2.0% and 4.0%, for the relative thermal conductivity in Fig. 5.

By taking the ratio of thermal-conductivity enhancement to the nanoparticle volume fraction, one obtains the reduced thermal-conductivity enhancement. In Fig. 6, comparisons of the reduced thermal-conductivity enhancement with respect to temperature are given for the same results used in Fig. 5. Our data show similar behavior with Refs. [6] and [16] in that the thermal conductivity of nanofluids is not much more temperature dependent than that of the base fluid. While on the contrary, Wang et al. [12] concluded in their study that the relative thermal conductivity of TiO<sub>2</sub>–water nanofluids is temperature dependent. Figure 6 shows that for the temperature range of

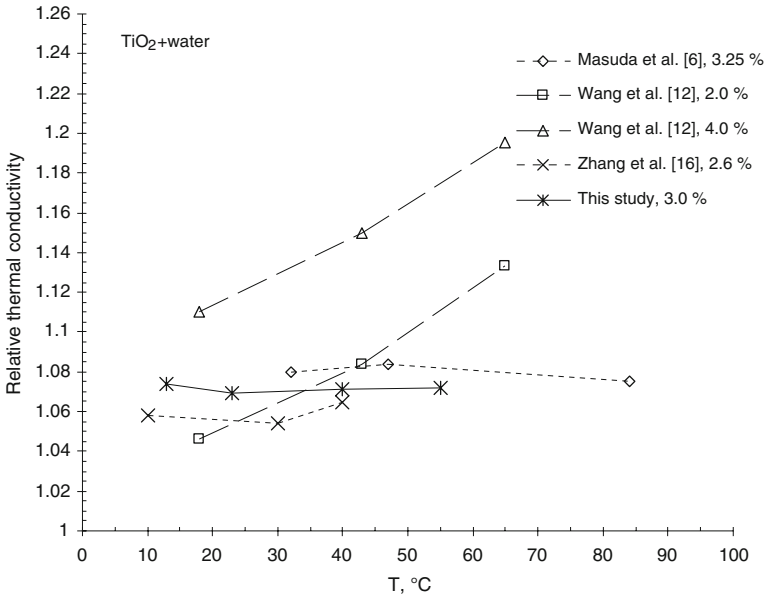


**Fig. 5** Temperature dependence of relative thermal conductivity of TiO<sub>2</sub>–water nanofluids

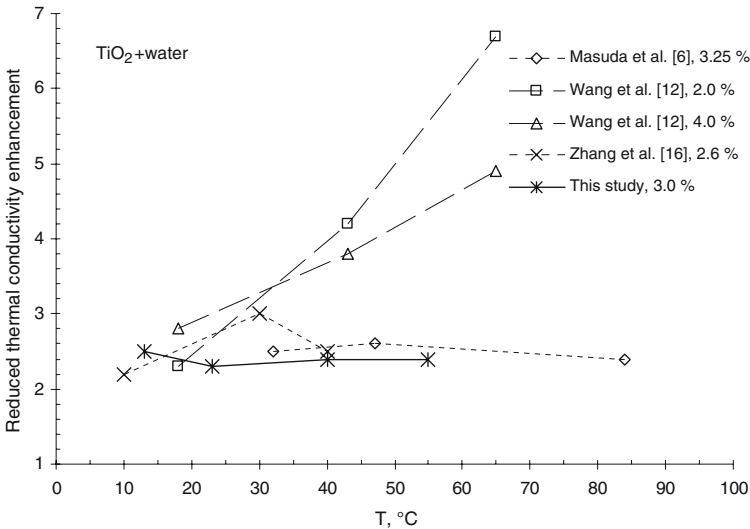


**Fig. 6** Comparisons of reduced thermal-conductivity enhancement versus temperature of TiO<sub>2</sub>–water nanofluids: results from the literature and this study

10 °C to 30 °C all reduced thermal-conductivity enhancement values are in the range of 2 and 3. For temperatures over 30 °C, our reduced thermal-conductivity enhancement values, the values of Masuda et al. [6] and Zhang et al. [16] are in the range of 2 and 3, whereas the results of Wang et al. [12] show an increase up to 7 at 65 °C.

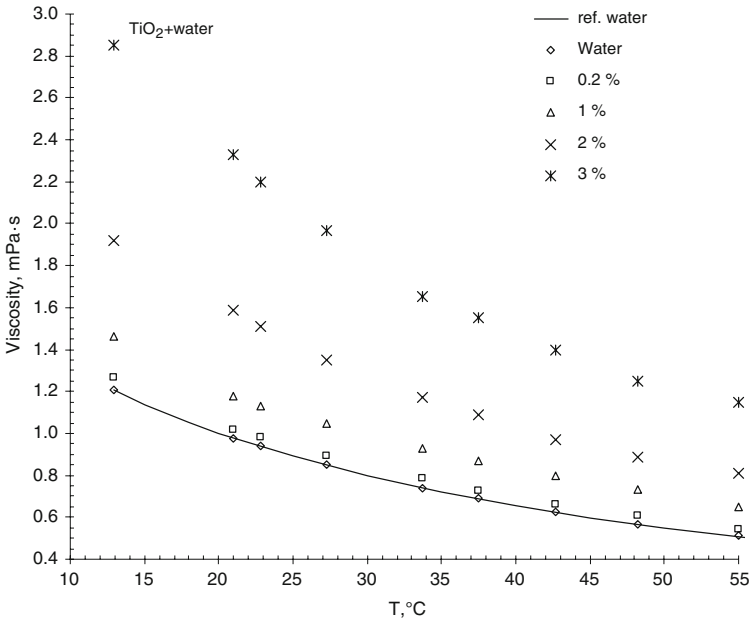


**Fig. 7** Effective viscosities of TiO<sub>2</sub>–water nanofluids from 0.2 vol% to 3 vol% as a function of temperature

### 3.2 Effective Viscosity of TiO<sub>2</sub> Nanofluids

To verify the accuracy of our system, the viscosity of water was measured before and after each experiment. The obtained results were compared with data from the literature [39]. After we performed the validation, the viscosities of nanofluids were measured for different particle concentrations, with temperatures between 13 °C and 55 °C. The results of these measurements are shown in Fig. 7, and the effective viscosity of TiO<sub>2</sub>–water nanofluids shows a similar behavior as water with increasing temperature.

Figure 8 gives the relative viscosity ( $\mu_r = (\mu_{\text{eff}})/(\mu_1)$ ), defined as the ratio of the effective viscosity of the nanofluid and the pure base fluid, as a function of volumetric particle concentration. Einstein proposed a viscosity correlation for a non-interacting particle suspension in a base fluid when the volume concentration is less than 5%.

$$\mu_{\text{eff}} = \mu_1 (1 + 2.5\phi) \tag{9}$$

where  $\phi$  is the volume fraction of particles.

Krieger and Dougherty [40] formulated a semi-empirical equation for relative viscosity expressed as

$$\mu_{\text{eff}} = \mu_1 \left( \frac{\phi}{\phi_m} \right)^{-[\eta]\phi_m} \tag{10}$$

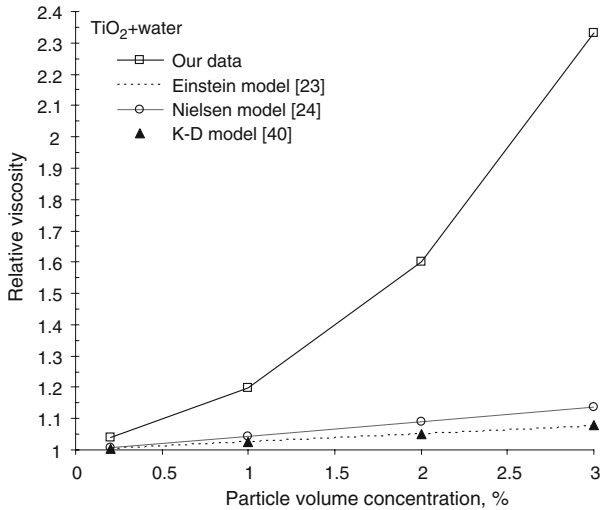


**Fig. 8** Relative viscosity of TiO<sub>2</sub>–water nanofluids as a function of nanoparticle volume fraction at 13 °C

where  $\phi_m$  is the maximum packing fraction and  $[\eta]$  is the intrinsic viscosity ( $[\eta] = 2.5$  for hard spheres). For randomly mono-dispersed spheres, the maximum close-packing fraction is approximately 0.64 [40].

Another model was proposed by Nielsen [24] for a low concentration of particles. Nielsen's equation is as follows:

$$\mu_{\text{eff}} = \mu_1 (1 + 1.5\phi) e^{\phi/(1-\phi_m)} \quad (11)$$

where  $\phi$  and  $\phi_m$  are the volume fraction of particles and the maximum packing fraction, respectively.

The measured viscosity of nanofluids is much higher than that predicted by the classical effective viscosity models, which shows the strong effect of interactions of the nanoparticles. The viscosity of nanofluids increases dramatically, with an increase in particle concentration which may be related to not using any surfactant or chemical additives while producing the nanofluids.

## 4 Conclusions

The thermal conductivity of TiO<sub>2</sub> nanoparticles in deionized water nanofluids was measured using a  $3\omega$  method for volume fractions ranging from 0.2% to 3.0%. The data showed that the thermal-conductivity enhancement was in relatively good agreement with the Hamilton–Crosser model. We also compared our results with the results of other researchers for the enhancement of the thermal conductivity of water-based nanofluids, containing TiO<sub>2</sub> spherical nanoparticles volumetric fractions between 0.2% and 3.0%; our results agreed within experimental error with the experimental results of Masuda et al. [6], Wang et al. [12], and Zhang et al. [16]. The

$3\omega$  measurement method for thermal conductivity was particularly well adapted as it required small amounts of sample size and was rapid and accurate (uncertainty within 2%). Measurements of thermal conductivity made at temperatures of 13 °C, 23 °C, 40 °C, and 55 °C showed that there is no dependence related to temperature; the thermal conductivity increased by the same order of magnitude as the base fluid which is water.

The effective viscosities of TiO<sub>2</sub>–water nanofluids with concentrations from 0.2 vol% to 3.0 vol% were measured at temperatures from 13 °C to 55 °C. The results show that for low volume additions of nanoparticles for 0.2% vol. fraction, the viscosity values follow quite well the viscosity values of pure water with a decrease in viscosity with increasing temperature and may be predicted by the Einstein law of viscosity. But, for higher additions of TiO<sub>2</sub> nanoparticles, the Einstein law of viscosity failed to explain the large increase in viscosity values. At 13 °C the increase was as large as two times that predicted by the Einstein law of viscosity for 3% vol. fraction.

**Acknowledgments** This work has been supported by TUBITAK (Project no: 107M160) and Agence Universitaire de la Francophonie (Project no: AUF-PCSI 6316 PS821).

## References

1. S.U.S. Choi, *Developments and Applications of Non-Newtonian Flows*, FED-231/MD-66 (ASME, New York, 1995), p. 99
2. W.H. Yu, D.M. France, J.L. Routbort, S.U.S. Choi, *Heat Transfer Eng.* **29**, 432 (2008)
3. S.M.S. Murshed, K.C. Leong, C. Yang, *Appl. Therm. Eng.* **28**, 2109 (2008)
4. J.C. Maxwell, *A Treatise on Electricity and Magnetism*, 2nd edn. (Clarendon Press, Oxford, UK, 1881), p. 435
5. R.L. Hamilton, O.K. Crosser, *Ind. Eng. Chem. Fundam.* **1**, 187 (1962)
6. H. Masuda, A. Ebata, K. Teramae, N. Hishinuma, *Netsu Bussei (Japan)* **7**, 227 (1993)
7. S.K. Das, N. Putra, P. Thiesen, W. Roetzel, *ASME J. Heat Transfer* **125**, 567 (2003)
8. H.E. Patel, S.K. Das, T. Sundararajan, A.S. Nair, B. George, T. Pradeep, *Appl. Phys. Lett.* **83**, 2931 (2003)
9. D. Wen, Y. Ding, *J. Thermophys. Heat Transfer* **18**, 481 (2004)
10. C.H. Chon, K.D. Kihm, *ASME J. Heat Transfer* **127**, 810 (2005)
11. C.H. Li, G.P. Peterson, *J. Appl. Phys.* **99**, 084314 (2006)
12. Z.L. Wang, D.W. Tang, S. Liu, X.H. Zheng, N. Araki, *Int. J. Thermophys.* **28**, 1255 (2007)
13. S.M.S. Murshed, K.C. Leong, C. Yang, *Int. J. Therm. Sci.* **47**, 560 (2008)
14. H.A. Mintsu, G. Roy, C.T. Nguyen, D. Doucet, *Int. J. Therm. Sci.* **48**, 363 (2008)
15. D.C. Venerus, M.S. Kabadi, S. Lee, V. Perez-Luna, *J. Appl. Phys.* **100**, 094310 (2006)
16. X. Zhang, H. Gu, M. Fujii, *Int. J. Thermophys.* **27**, 569 (2006)
17. B. Yang, Z.H. Han, *Appl. Phys. Lett.* **89**, 083111 (2006)
18. E.V. Timofeeva, A.N. Gavrilov, J.M. McCloskey, Y.V. Tolmachev, S. Sprunt, L.M. Lopatina, J.V. Selinger, *Phys. Rev. E* **76**, 061203 (2007)
19. R. Prasher, D. Song, J. Wang, *Appl. Phys. Lett.* **89**, 133108 (2006)
20. P.K. Namburu, D.P. Kulkarni, D. Misra, D.K. Das, *Exp. Therm. Fluid Sci.* **32**, 397 (2007)
21. J.H. Lee, K.S. Hwang, S.P. Jang, B.H. Lee, J.H. Kim, S.U.S. Choi, C.J. Choi, *Int. J. Heat Mass Transfer* **51**, 2651 (2008)
22. S.M.S. Murshed, K.C. Leong, C. Yang, *Int. J. Therm. Sci.* **47**, 560 (2008)
23. A. Einstein, *Investigations on the Theory of the Brownian Movement* (Dover, New York, 1956)
24. L.E. Nielsen, *J. Appl. Phys.* **41**, 4626 (1970)
25. A. Turgut, C. Sauter, M. Chirtoc, J.F. Henry, S. Tavman, I. Tavman, J. Pelzl, *Eur. Phys. J. Special Topics* **153**, 349 (2008)

26. M. Chirtoc, J.F. Henry, A. Turgut, C. Sauter, S. Tavman, I. Tavman, J. Pelzl, in Proceedings 5th European Thermal-Sciences Conference, ed. by G.G.M. Stoffels, T.H. van der Meer, A.A. van Steenhoven, Eindhoven (2008), ISBN 978-90-386-1274-4, MNH-12
27. M. Chirtoc, J.F. Henry, Eur. Phys. J. Special Topics **153**, 343 (2008)
28. H.W. Carslaw, J.C. Jaeger, *Conduction of Heat in Solids*, 2nd edn. (Oxford Univ. Press, London, UK, 1959)
29. D.G. Cahill, Rev. Sci. Instrum. **61**, 802 (1990)
30. M. Chirtoc, X. Filip, J.F. Henry, J.S. Antoniow, I. Chirtoc, D. Dietzel, R. Meckenstock, J. Pelzl, Superlattices Microstruct. **35**, 305 (2004)
31. D.S. Viswanath, T.K. Ghosh, D.H.L. Prasad, N.V.K. Dutt, K.Y. Rani, *Viscosity of Liquids* (Springer, New York, 2007)
32. D.H. Yoo, K.S. Hong, H.S. Yang, Thermochem. Acta **455**, 66 (2007)
33. Y. He, Y. Jin, H. Chen, Y. Ding, D. Cang, H. Lu, Int. J. Heat Mass Transfer **50**, 2272 (2007)
34. B.C. Pak, Y.I. Cho, Exp. Heat Transfer **11**, 151 (1998)
35. S.M.S. Murshed, K.C. Leong, C. Yang, Int. J. Therm. Sci. **44**, 367 (2005)
36. D. Wen, Y. Ding, IEEE T. Nanotechnol. **5**, 220 (2006)
37. D.A.G. Bruggeman, Ann. Phys., Leipzig **24**, 636 (1935)
38. H. Xie, M. Fujii, X. Zhang, Int. J. Heat Mass Transfer **48**, 2926 (2005)
39. D.R. Lide, CRC Handbook of Chemistry and Physics, 84th edn. (CRC Press, Boca Raton, FL, 2003)
40. I.M. Krieger, T.J. Dougherty, Trans. Soc. Rheol. **3**, 137 (1959)